Morphology of Isolated Triads

ROBERT D. MITCHELL, AKITSUGU SAITO, PHILIP PALADE, and SIDNEY FLEISCHER
Department of Molecular Biology, Vanderbilt University, Nashville, Tennessee 37235. Dr. Mitchell's present address is the Roche Institute of Molecular Biology, Nutley, New Jersey 07110. Dr. Palade's present address is the Department of Physiology and Biophysics, University of Texas Medical Branch, Galveston, Texas 77550.

ABSTRACT The triad is the junctional association of transverse tubule with sarcoplasmic reticulum terminal cisternae. A procedure for the isolation of highly enriched triads from skeletal muscle has been described in the previous paper. In the present study, the structural features of isolated triads have been examined by thin-section, negative-staining, and freeze-fracture electron microscopy. In isolated triads, key features of the structure observed in situ have been retained, including the osmiophilic "feet," junctional structures between the transverse tubule and terminal cisternae. New insight into triad structure is obtained by negative staining, which also enables visualization of feet at the junctional face of the terminal cisternae, whereas smaller surface particles, characteristic of calcium pump protein, are not visualized there. Therefore, the junctional face is different from the remainder of the sarcoplasmic reticulum membrane. Junctional feet as viewed by thin section or negative staining have similar periodicity and extend ~100 Å from the surface of the membrane. Freeze-fracture of isolated triads reveals blocklike structures associated with the membrane of the terminal cisternae at the junctional face, interjunctional connections between the terminal cisternae and t-tubule, and intragap particles. The intragap particles can be observed to be closely associated with the t-tubule. The structure of isolated triads is susceptible to osmotic and salt perturbation, and examples are given regarding differential effects on transverse tubules and terminal cisternae. Conditions that adversely affect morphology must be considered in experimentation with triads as well as in their preparation and handling.

The triad is composed of two different membrane systems, the transverse tubule and the terminal cisternae of sarcoplasmic reticulum, in junctional association (2–4). During excitation-contraction coupling in the muscle fiber, the signal for Ca^{++} release traverses this junction from t-tubule to terminal cisternae (5). As early as 1962 (6), periodic electron-dense structures were noted bridging the gap between the two types of muscle membranes. Franzini-Armstrong (7, 8) reported that these junctional "feet" (4) were arranged in repeating diamond-shaped units attached to one another at the corners. The major portion of each foot seemed to be more securely attached to the terminal cisternal portion of the triad (4, 7, 8). A variety of interpretations have been presented that suggest roles for the intragap material in excitation-contraction coupling (9–14).

In the companion paper (1), we described the isolation of purified triad structures from rabbit skeletal muscle. The present study deals with a description of the morphology of isolated triads and evaluates the susceptibility of triad structure to composition of the media, osmotic changes, and handling.

MATERIALS AND METHODS

Osmium tetroxide and glutaraldehyde (vacuum distilled in glass at low temperature and the distillate treated with a special grade of high surface active carbon and antacid to remove traces of glutaric acid) were obtained from Polysciences, Inc. (Paul Valley Industrial Park, Warrington, PA).

METHODS

Preparation of Triad Fractions

A rabbit skeletal muscle heavy microsome fraction, enriched in triads, was purified by one (Stage I) or two (Stage II) sequential 90-min gradient centrifugations to purify triads. A pyrophosphate mixture (20 mM $Na_4P_2O_7$, 20 mM NaH_2PO_4, and 1 mM $MgCl_2$, pH 7.1) was introduced to minimize aggregation referable to muscle proteins and to enhance purification. Two variants were described. The *standard* variant introduced the pyrophosphate mixture at the second gradient purification step, whereas the *pyrophosphate* variant made use of the pyrophosphate mixture throughout the entire isolation procedure, beginning with the homogenization of the muscle. Either variant resulted in high enrichment of triads with good retention of morphology, but some differences in enzymic properties were noted (1).

© The Rockefeller University Press · 0021-9525/83/04/1017/13 $1.00

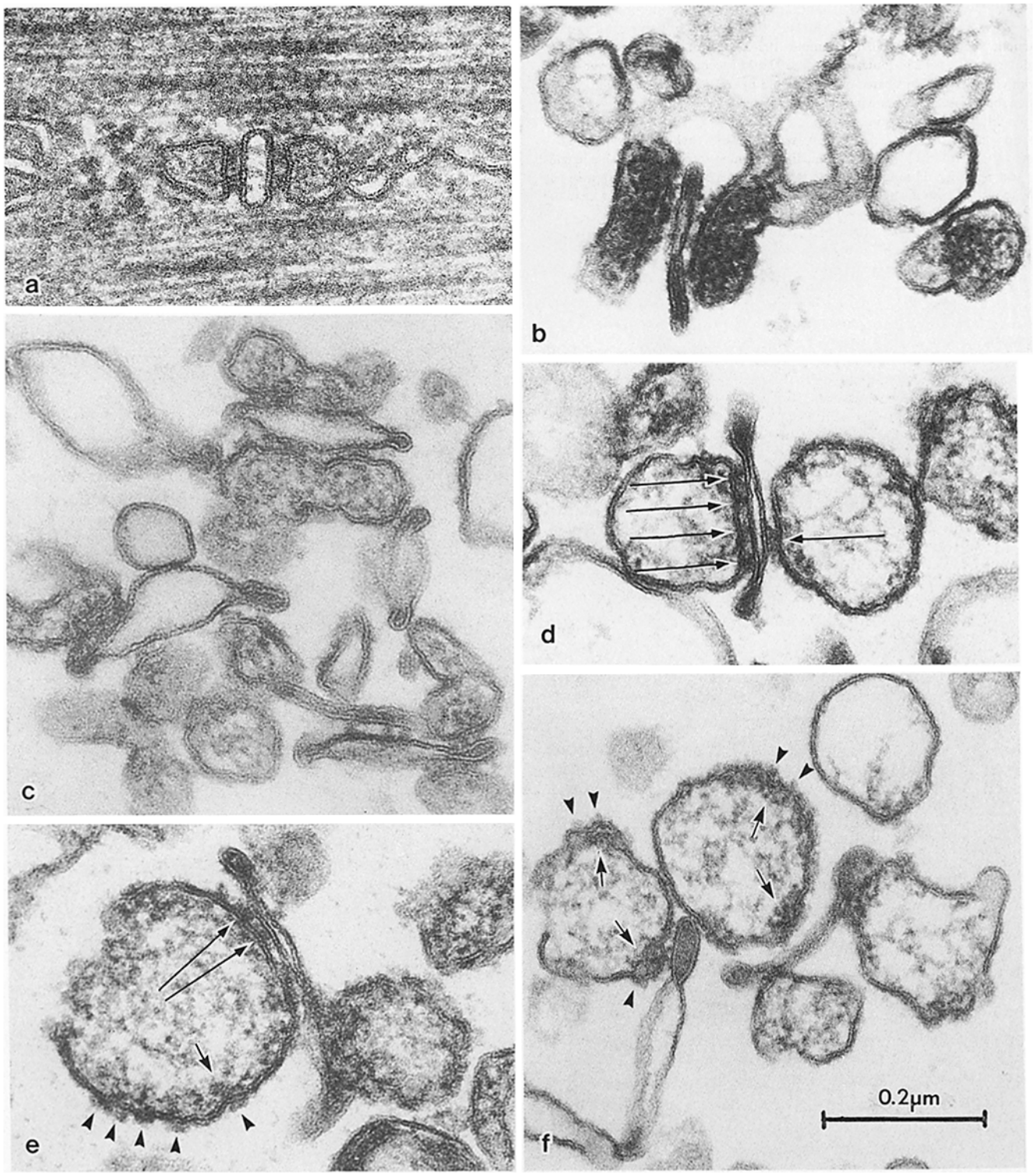

FIGURE 1 Triad structure observed in thin-section. (*a*) Cross-sectional view through a triad in rabbit skeletal muscle in situ. (*b* and *c*) Triad structures observed in *standard* Stage I preparations (1). Note the continuity of SR from opposing terminal cisternae in *b* and the extensive catenation of junctional elements in *c*. (*d*, *e*, and *f*) Triad structures observed in *standard* Stage II purified preparations (1). Junctional feet structures are observed on terminal cisternae both on junctional faces (arrows) as well as at former sites of junction attachment (arrowheads). Note regions of amorphous, electron dense patches associated with the inner face of the membrane within the terminal cisternae (short arrows). Feet can be observed on the external surface adjacent to patches of internally aggregated material. The contents of the terminal cisternae of Stage I *standard* triads (*b* and *c*) not exposed to pyrophosphate, are generally more condensed than seen for Stage II triads (*d*, *e*, and *f*), which have been treated with pyrophosphate. All micrographs × 140,000.

Electron Microscopy

Samples were routinely fixed in suspension directly from the gradient (in the sucrose and salt concentration in which they were isolated) in order to minimize osmotic shock. In general, the sample, 100–300 μg of protein, was fixed by addition of 0.1 vol 25% glutaraldehyde, 200 mM cacodylate, pH 7.2 (over ~15 s) with vortexing and incubated overnight (~12 h) at 0–5°C. Shorter fixation times were sometimes inadequate in that osmotic sensitivity was occasionally observed upon dilution after fixation.

For studies of structural lability, samples were challenged with putative osmotic perturbants by soaking in media containing solutes for variable lengths of time and then diluting away from the effector, either rapidly (15 s) or slowly (up to 12 h). Fixation and subsequent centrifugation were carried out in cellulose nitrate tubes of Beckman swinging bucket rotors (types SW41, SW56, SW50).

For in situ studies, rabbit skeletal muscle tissue (small cubes, 0.3–0.5 mm on a side) was fixed on ice for 2 h in a solution of 2.5% glutaraldehyde in 8% sucrose, 0.1 M sodium cacodylate buffer (pH 7.2).

PREPARATION FOR THIN SECTION: After completion of primary fixation, samples were diluted, pelleted, and washed with 0.1 M cacodylate buffer, 0.3 M sucrose to remove residual glutaraldehyde. Subsequent postfixation of both whole tissue and pelleted fractions was performed on ice using 1% OsO_4 in Michaelis buffer (15): 2 h for tissue and 2–12 h for pellets. Samples were then "block-stained" with 0.5% uranyl acetate, pH 6.0 for 2–3 h at room temperature, followed by dehydration with a graded ethanol-water series. Cellulose nitrate was then removed with propylene oxide, and samples were embedded in Epon 812. Thin-sections were obtained on an LKB Ultratome (LKB Instruments, Rockville, MD), stained with 1% uranyl acetate in 50% ethanol for 10 min, and counter-stained with lead citrate (16). The samples were examined in either a JEOL JEM-100S or Hitachi HU-11B electron microscope.

PREPARATION FOR NEGATIVE STAINING: Although several other reagents including uranyl acetate and ammonium molybdate were used for negative staining, only phosphotungstic acid (PTA) was found to consistently produce a high contrast presentation of triad fine structure. Samples were prefixed overnight in 2.5% glutaraldehyde before negative staining with 1% PTA, as described previously (15).

PREPARATION FOR FREEZE-FRACTURE: Freeze-fracture and replica preparation were carried out using a Balzers BAF 3000 apparatus (Balzers High Vacuum Corp., Santa Ana, CA) as described by Deamer and Baskin (17). Samples of triads were prefixed with 2.5% glutaraldehyde as described above for isolated triads. Pelleted samples were covered with a solution containing 25% glycerol, 5 mM HEPES (pH 7.2), 100 mM KCl and 0.3 M sucrose and infiltrated for 2–3 h before the freeze-fracture process. Rabbit skeletal muscle tissue was sectioned into cubes and glutaraldehyde-fixed as described above for in situ studies. The cubes were washed with 0.1 M cacodylate, 8% sucrose for 2–3 h, and immersed in a solution of 25% glycerol in 0.1 M cacodylate for 2–3 h. Samples were mounted on gold disks and frozen in FREON 22. Both whole tissue and isolated material were fractured at −110°C and immediately shadowed with 200-Hz frequency change Pt/C (~2 mm thickness) and backed with carbon.

RESULTS

Morphological Features of Isolated Triads

THIN SECTION VIEWS: Triad structures in situ are readily identified in thin section. The terminal cisternae of the sarcoplasmic reticulum (SR), which contain intracompartmental osmiophilic material, are junctionally associated with invaginations of the surface membrane known as transverse tubules (Fig. 1 *A*). Close proximity of terminal cisternae to transverse tubule is maintained by rows of periodic osmiophilic junctional structures, or "feet" (4), bridging the gap between the two membranes. The triadic gap is relatively uniform in width, within the realm of characteristic scalloping. The repeat distance from center to center of adjacent feet is also quite constant (Table I).

Isolated purified triads exhibit similar morphological features (Fig. 1). The gap of the junction after isolation remains approximately uniform in width (Fig. 1 *b* and *c*) and is comparable with that seen in situ (Table I). Where seen, the most prominent feature of the junction of the isolated triad is the periodic arrangement of osmiophilic feet. The feet of isolated triads have an average center-to-center repeat distance of 285 Å, comparable to that seen in situ (Table I). They appear as discrete entities varying in width from 125 to 250 Å with a space between adjacent feet of 125–200 Å (Fig. 1). This variation probably reflects their shape and arrangement. Therefore, an upper limit of ~250 Å represents their "diameter." Feet are also observed on terminal cisternae surfaces which are associated only with the terminal cisternae and no longer with the t-tubule (arrowheads in Fig. 1 *e*). The feet extend an average of ~100 Å from the surface of the membrane, about the same whether or not they are still associated with the junction (Table I). It would appear that some of the junctions become disrupted during isolation, resulting in loss of attachment to t-tubule. Feet have not been observed attached to free transverse tubule. Thus, under conditions of isolation, feet are more tightly associated with the terminal cisternae than with the transverse tubule.

Frequently, the appearance of the isolated triad structure is that of a symmetrical "butterfly" configuration (Fig. 1 *b* and *d*) with two apposing terminal cisternae junctionally linked to the central flattened t-tubule. However, a wide range of other geometric configurations has been encountered in isolated triads. For instance, two and possibly three terminal cisternae appear attached to t-tubules in Fig. 1 *e* and *f*. Two cisternae can be seen on the same side of the transverse tubule in a cis-like configuration (Fig. 1 *f*) while cisternae can also be observed junctionally associated diagonally opposite in a more trans-like arrangement (Fig. 1 *e*). Dyad configurations (i.e. one cisterna per tubule) and multiple cisternal attachments to individual t-

TABLE I

Dimensions of Junctional Structures (Feet) and Gap Spacing of the Triad Junction

	Gap spacing (Å)	Junctional structures (feet) (Å)		
			Width*	
		Repeat distance	Triad-associated	Terminal cisternae-associated
A. Thin section‡				
In situ	117 ± 17 (54)	279 ± 45 (51)	108 ± 17 (54)	Not observed
Isolated triads	108 ± 25 (109)	284 ± 49 (113)	100 ± 23 (168)	106 ± 28 (127)
B. Negative staining				
Isolated triads	171 ± 22§ (54)	279 ± 45 (205)	112 ± 17 (84)	116 ± 17 (159)

* Distance the junctional structure extends out from the surface of the terminal cisternae membrane.

‡ The samples were prepared for thin section by glutaraldehyde fixation followed by OsO_4 staining. The gap spacing is the spacing between junction from the transverse tubule to terminal cisternae membranes as measured across the feet. The values in parentheses refer to the number of measurements. Values for isolated triads include determinations from Stage I and Stage II preparations of both variants (1).

§ Negative staining tends to separate the junction. The value is the average of closest distance of the junction which has been retained. Therefore, this value is probably an overestimate and not as reliable as that obtained from thin section.

tubules (e.g., Figs. 1*c* and 8*e*) are also seen. In addition, multiple t-tubule attachments to single terminal cisternae are often seen (Fig. 1*c* and *f*). The basis for the multiple attachments may be explained by (*a*) known branching of t-tubules (18), which is not readily observed in thin section and/or (*b*) the possible reassociation of junctions that may have separated during isolation. Multiplicity of attachment is particularly extensive in some fields (Fig. 1*c*), indicating chaining or catenation of several junctional complexes. In rare instances in thin section (Fig. 1*b*), portions of SR can be seen extending from the terminal cisternae, indicating continuity between the two terminal cisternae on opposite sides of the transverse tubule.

Sample pretreatment can be reflected in the appearance of the isolated triads. The two variants of triad isolation (1) make use of two sequential sucrose gradient purifications steps. In the *standard* variant the first gradient has no pyrophosphate, but the second one does. The contents of the terminal cisternae of *standard* variant Stage I triads (Fig. 1*b* and *c*) appear more condensed than in situ (Fig. 1*a*) and more electron dense and uniformly distributed than in the *standard* variant Stage II final product (Fig. 1 *d*, *e*, and *f*), which has been treated with pyrophosphate mixture. For the latter, the internal contents of the vesicles appear less compact and segregate into two components: (*a*) randomly distributed amorphous material and (*b*) electron-dense patches preferentially located at the inner face of portions of the terminal cisternae membrane which display feet on the external face. *Standard* and *pyrophosphate* Stage II variants are practically indistinguishable in appearance (1).

NEGATIVE STAINING: Phosphotungstate gave better contrast than uranyl acetate or ammonium molybdate. The triad structure observed by negative staining (Fig. 2) reflects more of a three-dimensional view than that seen with thin-section electron microscopy. The t-tubule sometimes appears entirely surrounded, not only by terminal cisternae at the junctional faces, but also at the ends by SR that is continuous with the opposed terminal cisternae (Fig. 2*a* and *b*), as seen in thin section (Fig. 1*b*) and in situ (19). Triad structures can be observed containing portions of the lateral cisternae of SR continuous with the terminal cisternae via narrow processes (Fig. 2*b–d*) giving rise to characteristic fenestrations (2). Such structures are not so readily observed in thin-section, which gives only a two-dimensional view in the plane of the section.

In general, the junctional gap spacing is widened by the conditions of pretreatment and drying associated with the negative-staining procedure (Table I). Nevertheless, negative staining, especially in more separated junctions, gives additional insight to the junctional structures (Fig. 2*c* and *d*) as compared with thin-section electron microscopy. Junctional structures preferentially remain associated with the terminal cisternae even when separated away from the t-tubule. The junctional structures in negative staining appear identical to the feet observed in thin section. They extend about 100 Å from the surface in repeat units of ~280 Å (Table I). The junctional feet appear somewhat flared, approximating a trapezoid with a width of 240–300 Å. The junctional surface of the terminal cisternae has a scalloped appearance with the feet anchored at the hills rather than in the valleys (Fig. 2*c*). The junctional surface (Fig. 2*c* and *d*) does not appear to contain the 30–40 Å surface particles that are characteristic of the remainder of the SR surface (Fig. 2*d*, encircled area). The lack of particles can be noted especially in the valleys, where there is relatively smooth surface appearance. Hence, the junctional surface is distinctly different from the remainder of the SR membrane.

The uneven stain penetration through feet (Fig. 2*c*, encircled area) further suggests that they are composed of stalked globular subunits. A 20–30-Å wide strand of material has been observed running parallel to the terminal cisternal membrane surface (Fig. 2*c*, circled zone), perhaps serving to attach adjacent feet at their flared tops. No such discrete entity is seen in most micrographs, but the adjacent feet often appear associated as though connected.

The surface of the transverse tubule generally has a smooth appearance, although in rare instances some surface material without clearly defined structure can be observed (Fig. 2*d*, open arrowheads).

FREEZE-FRACTURE: Isolated triad structures can also be visualized, in glutaraldehyde-fixed samples, by freeze-fracture electron microscopy. The p and e fracture faces of the SR are readily distinguished by the high particle density on the p face (17, 20). In many cases, closely apposed terminal cisternae and t-tubule are observed without clear evidence of bridging structures within the triadic gap. However, the probability that the fracture plane would transect the gap to correctly expose the junctional feet is small.

New junctional detail is revealed in isolated triads by freeze-fracture. A striking characteristic of the junctional face of the terminal cisternae is the rectangular blocklike structures observed in the isolated triad in Fig. 3*a*. Comparison with the junctional structures of the triad observed by negative staining at the same magnification (Fig. 3*b*) suggests a similar periodicity and thickness to the blocklike structures (Fig. 3*a*). In some cases the blocks appear to be composed of doublets, suggestive of subunit structure (lowermost arrowheads in Fig.

FIGURE 2 Negative staining of isolated triads. The fraction was prepared by the *standard* variant, Stage I (1). (*a*) Low field magnification of isolated triad material prefixed with glutaraldehyde and visualized with phosphotungstate. × 90,000. Readily identifiable junctional structures can be observed in several triads. (*b*) Isolated triad structure with associated lateral cisterna (*LC*). The negative staining enables visualization of the continuity of SR from opposite sides of the transverse tubule, which gives the appearance of the transverse tubule being encircled by SR. × 90,000. The lateral cisterna can be observed to be attached to terminal cisternae (*TC*) via fenestrations. (*c*) The scalloped appearance of the junctional surface is readily seen by negative staining on both junctional faces of the terminal cisternae. The terminal cisterna on the left is continuous with less electron-opaque lateral cisterna. Three structural components can be observed in the triad junction and are illustrated in the small encircled area. The components are: (*a*) junctional structure, associated with the membrane surface of the terminal cisternae and extending about 100 Å normal to surface; (*b*) an intermediate thin strandlike component ~25–30 Å wide; and (*c*) some amorphous material which may extend from the transverse tubule (*tT*) and associate with the other components. Only the junctional structure is regularly observed, and it also shows indications of stalked globular subunit structure in the encircled area. × 400,000. (*d*) Some t-tubule associated material is designated (open arrowheads). Surface particles characteristic of calcium pump protein can be observed on the surface of nonjunctional SR (encircled area) but not at the junctional surface. Note, especially the valleys of the scalloping which are devoid of such surface material. × 400,000.

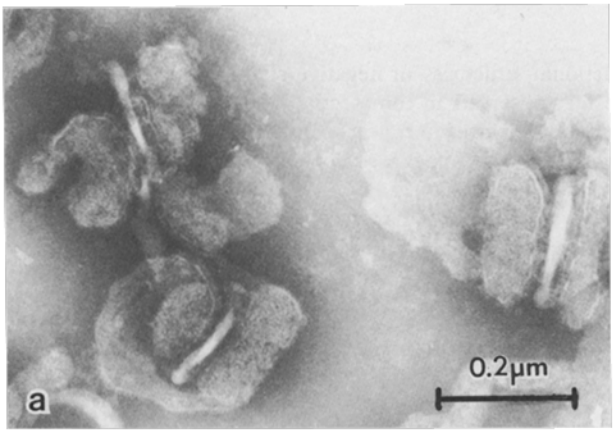
0.2μm
a

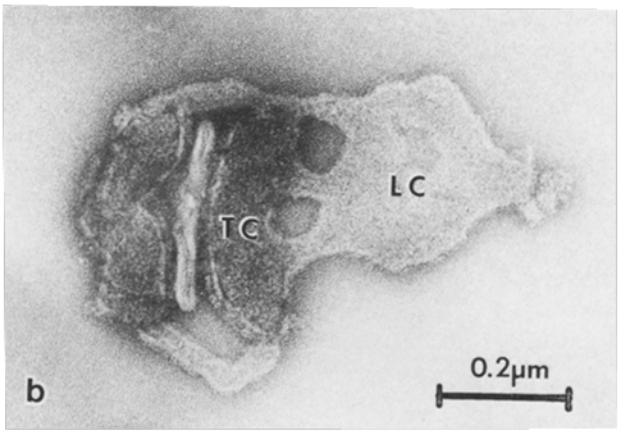
LC
TC
0.2μm
b

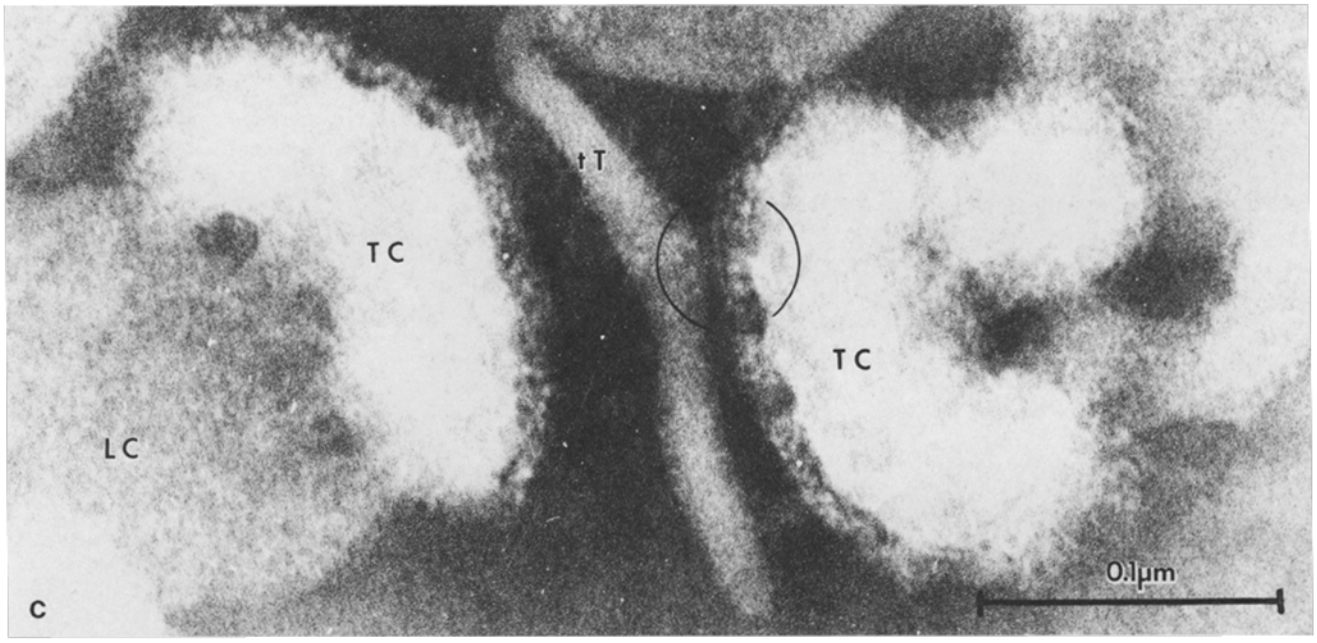
tT
TC
TC
LC
0.1μm
c

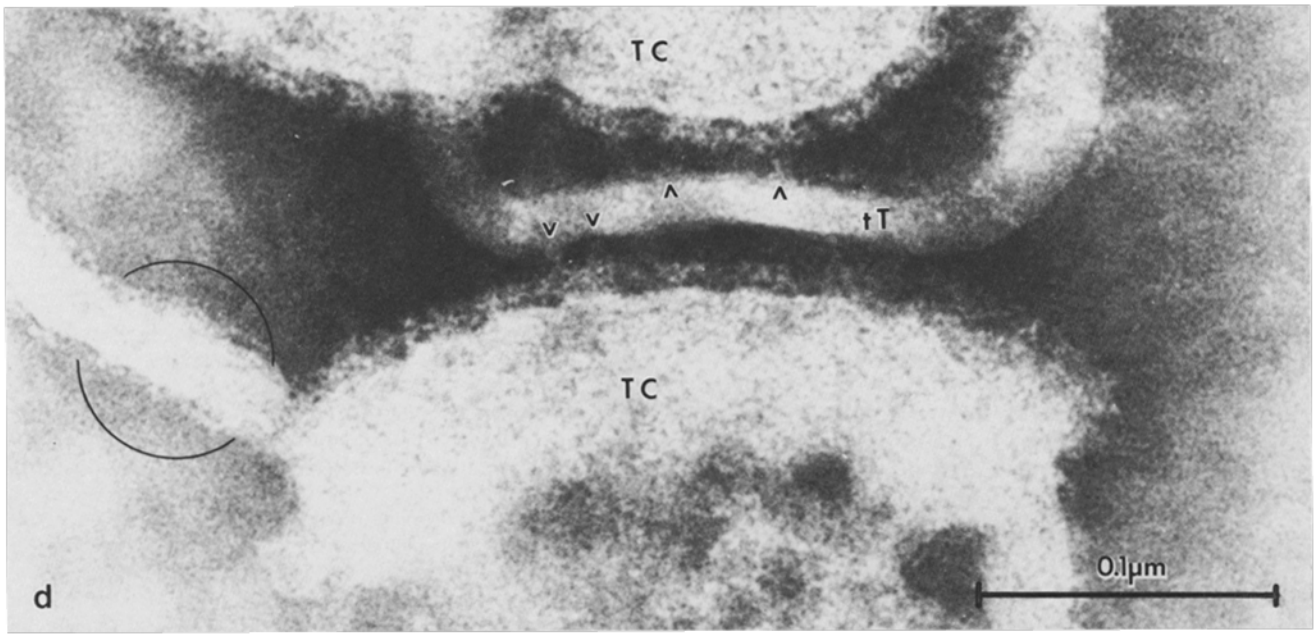
TC
v v
^ ^
tT
TC
0.1μm
d

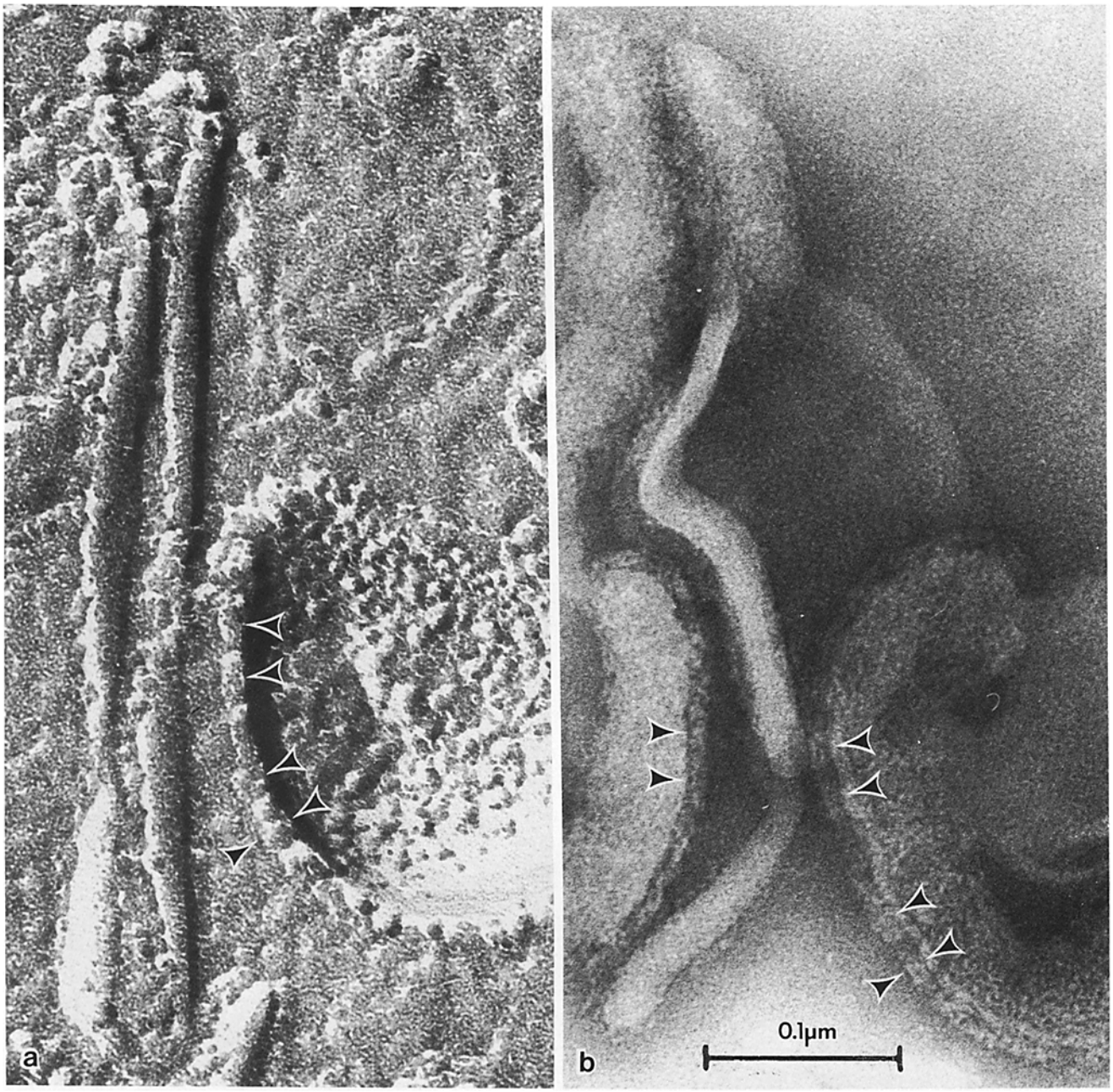

FIGURE 3 Triad ultrastructure compared by freeze-fracture and negative staining. The emphasis is on the junctional face of the terminal cisterna denoted by multiple arrowheads. The junctional structures, as observed by negative staining, display similar periodicity to the rectangular blocklike structures seen by freeze-fracture. In both cases the fraction used was Stage I triad-enriched material of the *standard* variant. × 300,000.

FIGURE 4 Freeze-fracture electron micrographs of triads, both isolated and in situ. (*a*) A catenated triad consisting of at least three transverse tubules and multiple terminal cisternae. This sample was prepared by the *pyrophosphate* variant, Stage II (1). The *e* and *p* faces of sarcoplasmic reticulum are indicated. Two features of the triad junction can be observed in this complex triad: (*i*) rectangular blocks (▲); and (*ii*) interjunctional associations between t-tubule and terminal cisternae (clearly observable in the circled area) are somewhat varied in appearance. Such variation in appearance undoubtedly reflects the nature of the fracture. (*b*) A triad with intragap structures associated with the t-tubule (left face). The intragap structures have diverse shapes and periodicity (⋀). Thusfar, freeze-fracture is the only method of sample preparation that unmistakably reveals association of particles with the transverse tubule. Triads in *b* and *c* were prepared by the *standard* variant (Stage I). (*c*) The transverse tubule on the left shows particles (⋀) aligned on both sides with a periodicity of ~280 Å. This is the same periodicity observed in thin sections referable to the junctional feet. In the triad on the right, intragap structures are seen, aligned in the direction of the junction (⋀). In situ micrographs are shown in *d* and *e*. (*d*) A row of periodic blocklike structures (▲) is observed in the gap between the t-tubule (*tT*) and the *SR* extending from the region of the *SR* terminal cisternae *e* face, to the *p* face, with which face they appear to be more closely associated. Some smaller particles decorate the t-tubule with similar periodicity (⋀). These particles have the same appearance as that observed in the isolated triads (*c*). (*e*) The junctional face of the terminal cisternae contains the characteristic blocklike structures (▲) (compare with Fig. 3). The smaller intragap particles closely associated with transverse tubule can likewise be observed (⋀). There is the suggestion of pairing of blocklike structures with the intragap particles. Note especially where the sets of symbols are apposed. All micrographs × 140,000.

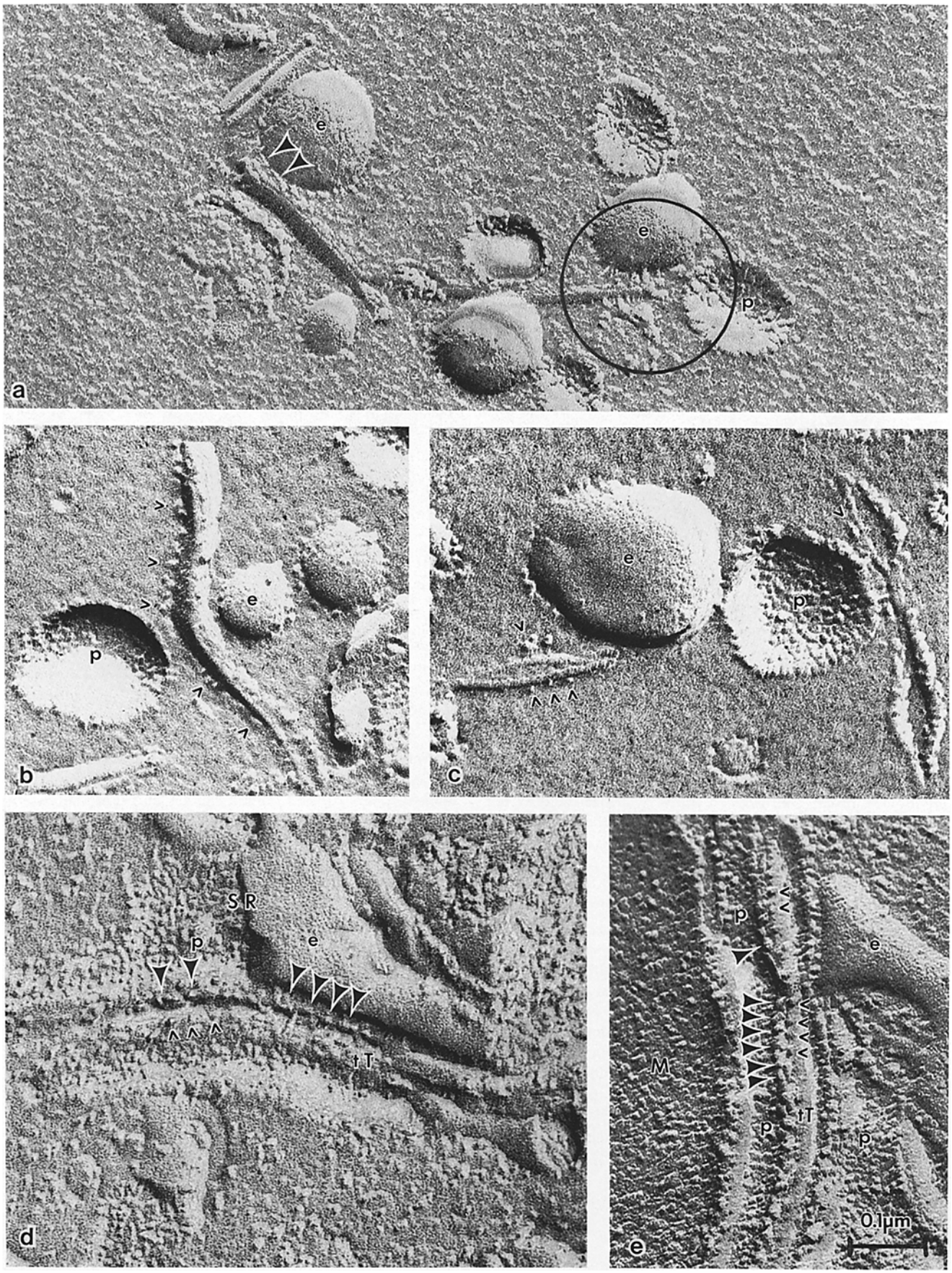
a
e
e
p
b
e
p
c
e
p
d
SR
p
e
tT
e
p
M
tT
p
p
0.1μm

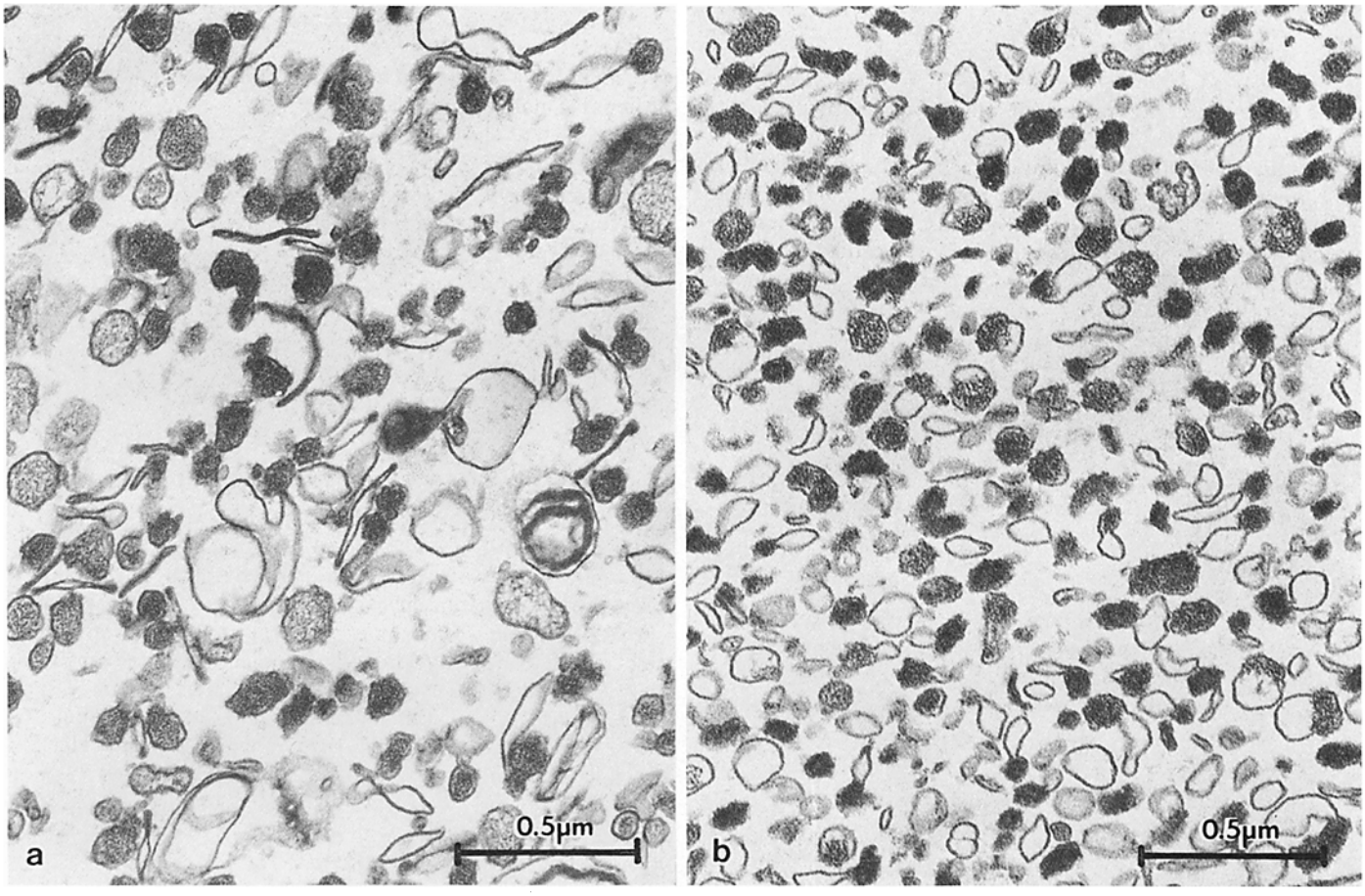

FIGURE 5 Osmotic effect of sucrose on triads. (a) Stage I enriched triads were isolated according to the *standard* variant (1). The sample was fixed with glutaraldehyde directly from the gradient in 35–40% sucrose (× 50,000). The morphology of the triads is well preserved. (*b*) Same sample as in (a) osmotically shocked by rapid dilution from high sucrose medium. *Standard* Stage I material was stored overnight in 40% sucrose in the cold, then rapidly diluted to 10% sucrose. 15 s later the sample was fixed with glutaraldehyde. × 50,000. Preferential swelling of the transverse tubule portion of the structure may be noted.

3 *a*, left-most arrows in Fig. 3 *b*).

Several types of structures appear to be associated with the junction as revealed in isolated triads by freeze-fracture: the rectangular blocklike structures (mentioned above - bold arrowheads) that are clearly associated with the terminal cisternae membrane (Figs. 3 *a* and 4 *a*); intragap particles (open arrowheads, Fig. 4 *b* and *c*) that reside within the junctional gap in closer association with the t-tubule; and interjunctional structures that appear to connect terminal cisternae with t-tubule (Fig. 4 *a*).

Freeze-fracture replicas of skeletal muscle, although complicated by the myriad of other components that are present in the muscle fiber, also reveal junctional detail of the t-tubule-sarcoplasmic reticulum system. Seemingly comparable junctional structures can be found in situ (Fig. 4 *d* and *e*); including both periodic rectangular blocks, some with subunit structure; and intragap particles. In some instances, juxaposition is suggested between the terminal cisternae-associated blocklike structures and the intragap particles, more closely linked to the t-tubules, (Fig. 4 *e*, apposed symbols).

Susceptibility of Triad Morphology to Osmotic Perturbation and Salt

OSMOTIC SENSITIVITY TO SUCROSE: Isolated triads have been found to be severely affected by sudden changes in sucrose concentration. Fig. 5 *a* illustrates *standard* Stage I enriched triadic material (1) fixed directly from the gradient in 40% sucrose. Tubules remain slender and terminal cisternae densely packed, even compressed, compared with that in situ (Fig. 1 *a*). When this fraction is incubated for 12–15 h in the cold and the sucrose concentration is abruptly reduced to ~10% by acute dilution, with prompt fixation with glutaraldehyde, the transverse tubules appear preferentially swollen, whereas the terminal cisternae remain largely unchanged with contents densely packed (Fig. 5 *b*).

Swelling of transverse tubule is not observed when the sucrose concentration is reduced immediately after collection of the sample from the gradient (<2 h of exposure to high sucrose in Stage I or II gradient centrifugations). Swelling of the t-tubule is also not obtained when the sample remains in high sucrose for 12–15 h and is then fixed without dilution of sucrose (not shown). We conclude that sucrose is slowly permeable, requiring many hours to equilibrate across the t-tubule membrane in the cold.

SENSITIVITY TO SALT: The presence of pyrophosphate causes some swelling of the terminal cisternae. This can be appreciated by comparing the morphology of Stage I triad-enriched material (1) prepared by the *standard* variant (Fig. 6 *a*) vs. the *pyrophosphate* variant (Fig. 6 *b*). Both fractions were fixed promptly after collection from the gradient. The contents of the terminal cisternae of the *standard* variant appear some-

what more densely packed than in situ (Fig. 1 *a*), whereas in the *pyrophosphate* variant they appear more swollen. This difference is attributable to exposure to pyrophosphate since the terminal cisternae of purified triads prepared by the *standard* variant of the Stage II gradient (1), which contains pyrophosphate mixture, also appear dilated (e.g., Fig. 1 *d*, *e*, and *f*). Otherwise, the transverse tubule appearance and junctional associations are similar for both variants. In general, exposure to pyrophosphate at either stage of purification results in dilated terminal cisternae, but longer exposure seems not to further alter the morphology.

High salt, such as 0.7 M KCl, has a disastrous effect on triad morphology (21). Even though fractions purified using KCl are highly enriched in a t-tubule marker enzyme such as adenylate cyclase activity (1), triad morphology is appreciably disrupted (not shown). Procedures employing high KCl concentrations in the purification of triad material result in general alterations of triad morphology, especially swelling and rupture of the terminal cisternae, as evidenced by selective loss of contents (21).

High salt also seems to partially extract the junctional feet. Progressive extraction with increasing salt concentration is illustrated in Fig. 7 as viewed by negative staining. 2-h treatment of triads with KCl concentrations as low as 0.1 M (Fig. 7 *b*) already causes some loss of the junctional structure detail as viewed by negative staining. The junctional feet progressively lose more definition with increased salt concentration (Fig. 7 *c* and *d*).

KCL-INDUCED OSMOTIC SWELLING OF TRANSVERSE TUBULE: Osmotic perturbation by KCl was tested on isolated transverse tubule. A triad fraction prepared by isopycnic centrifugation (21) was preincubated for 1 h in 50% sucrose, 0.7 M KCl and floated upwards by centrifugation (1.5 h) into lower concentration sucrose containing either 0.7 M KCl (Fig. 8 *a*) or no KCl (Fig. 8 *b*). A fraction containing transverse tubule[1] was collected at a lower density of sucrose. The t-tubules in the fraction that experienced decreased external KCl and sucrose became swollen (Fig. 8 *b*, arrows), while those in the control, experiencing only reduction in sucrose concentration (Fig. 8 *a*), were not. These results show that KCl, like sucrose, was able to produce osmotic swelling of isolated transverse tubule, although KCl is more readily permeable than sucrose since shorter preincubation in KCl was sufficient to elicit the osmotic swelling.

Swollen transverse tubule structures have a characteristic appearance, approximating a balloon with nipplelike tips pinched off at opposite poles of the vesicles. The nipples are filled with aggregated osmiophilic material (Fig. 8 *b*). Such tips have been previously reported in transverse tubule fractions by Lau et al. (22) and are now also observed in transverse tubule within the triad structure (Figs. 1, 5, and 6). The visualization of these electron-dense nipples appears to be a diagnostic for isolated transverse tubule which discriminates it from light SR, especially when the latter takes on a flattened appearance such as in high sucrose medium. The tips can also be observed in freeze-fracture (Fig. 3 *a*).

There does not appear to be preferential attachment of terminal cisternae to the nipples as compared with the main body of the transverse tubule. Occasionally, transverse tubular profiles are encountered in which these sites of aggregated material are viewed at roughly periodic (0.1–0.2 μm) intervals (Fig. 8 *c*, *d*, and *e*). Some osmiophilic material has been observed within t-tubule of triads in situ (Fig. 1 *a*), although this material is more closely spaced.

[1] The use of KCl to separate transverse tubule from terminal cisternae results in only a small yield of free transverse tubule.

DISCUSSION

The muscle fiber is densely packed with a variety of structures that complicate the visualization of triad junctional detail. The availability of purified triads simplifies their study. This report describes the morphology of isolated triads observed by three different methods of sample preparations and the influence of a variety of conditions that perturb their structure.

Morphology of the Triad Structure

Triad junctions in situ exhibit a number of well-documented morphological features. The most obvious is the close apposition of pairs of terminal cisternae aligned on either side of the long slender transverse tubule. Homogenization of the tissue pinches off portions of the transverse tubule, giving rise to triads. In this context, we use the term triad to refer to any numerical combination of terminal cisternae junctionally associated with transverse tubule, rather than to limit the term to two terminal cisternae properly apposed and junctionally linked to a single transverse tubule. In the limit, the smallest triad unit is a single terminal cisterna apposed to a t-tubule. Dyad units of this form have been reported in mammalian skeletal muscle in situ (23). More extensive associations of terminal cisternae with t-tubules may result from t-tubule branching and/or possibly reassociation (24, 25) during isolation. During homogenization some of the sarcoplasmic reticulum pinches off. More frequently, the terminal cisternae are preferentially retained in isolated triads, although on occasion some of the lateral cisternae remain attached via fenestrated connections (Fig. 2). Retention of such large multicomponent structures attests to the gentleness of the isolation procedure (1).

This is the only detailed comparison of isolated triads by three methods of sample preparation for electron microscopy. The isolated triads are readily discernible by each of the methods. The key features described were retained in both the enriched (Stage I) and more purified triad fractions (Stage II), except where noted.

The feet structures can be observed in regions of the terminal cisternae that are no longer junctionally associated, but that are referable to junctional surface. Such feet structures have been previously observed, but only when tannic acid enhancement was used (26, 27). The junction observed by thin section in isolated triads is similar in gap spacing and in ultrastructural detail to the feet observed in situ (Table I). Our studies are the first to observe isolated triads by negative staining. Both thin section and negative staining show identifiable junctional structures extending ~100 Å (Table I). Both have the same periodicity as well.

The junctional structure observed by negative staining and the junctional feet seen in thin section appear to be one and the same, based on their similar location in the triad junction, width, and periodicity. Subunit structure is suggested by the negative staining. The fine strand observed in negative staining (Fig. 2 *c*), running parallel to the membrane, may be different from a medial line reported in thin section (28–30). The latter is located at the center of the junction, whereas that seen by negative staining displays a proximity closer to the t-tubule side of the junction (Fig. 2 *c*). In our isolated triads, we find

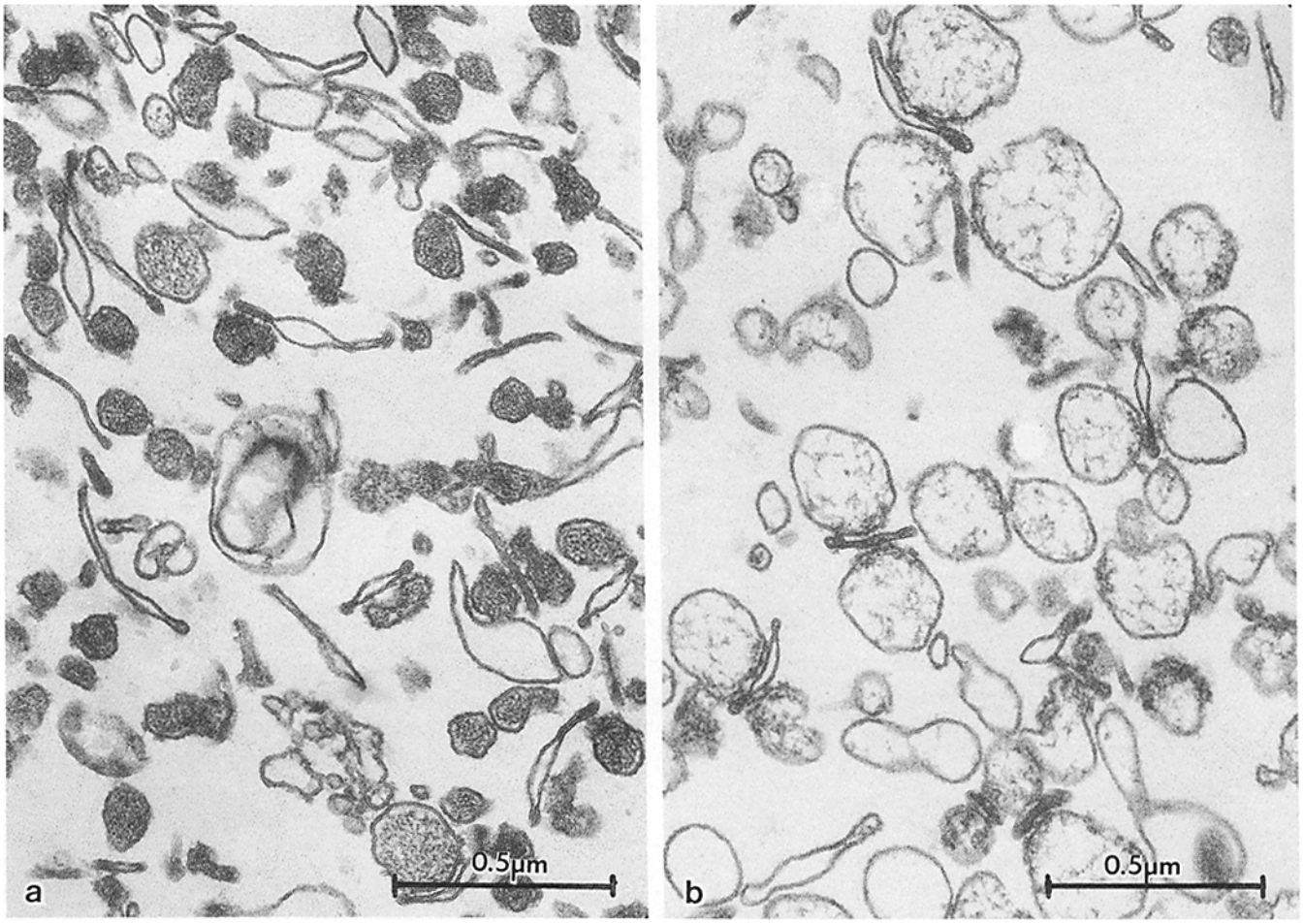

FIGURE 6 Effect of pyrophosphate mixture on triad appearance. Stage I enriched triad material (1) isolated (*a*) by the *standard* variant in the absence of pyrophosphate as compared with *b*, by the *pyrophosphate* variant, prepared in the presence of pyrophosphate mixture in all media from homogenization through Stage I gradient. Note the more condensed state of the contents of the terminal cisternae from the *standard* vs. the swollen appearance of the *pyrophosphate* variant. × 60,000. The terminal cisternae in situ (Fig. 1 *a*) is intermediate between the more condensed and swollen appearance of the two isolated variants.

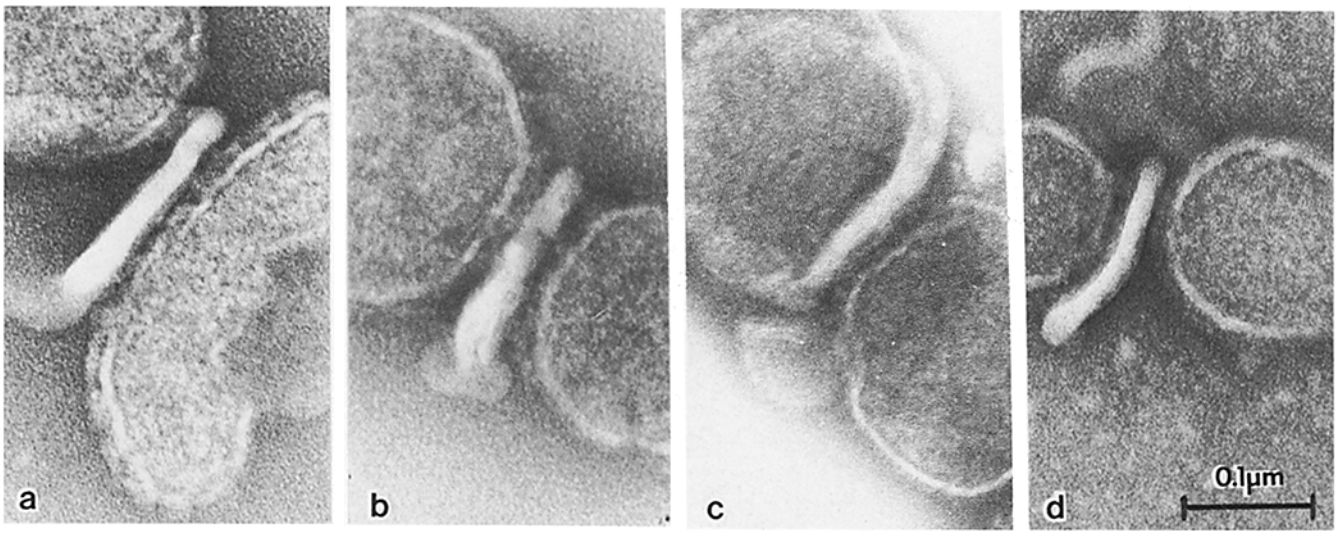

FIGURE 7 Sensitivity of junctional feet structure to KCl concentration of the medium. The triad fraction (Stage 1, *standard* variant (1) was preincubated on ice for 2 h before the usual 12-h fixation with glutaraldehyde and subsequent negative staining: (*a*) no KCl (*b*) 0.1 M KCl (*c*) 0.3 M KCl, (*d*) 0.7 M KCl. Although transverse tubules and terminal cisternae remain associated, a progressive degradation of the bridge structure can be observed as the salt concentration is increased. × 175,000.

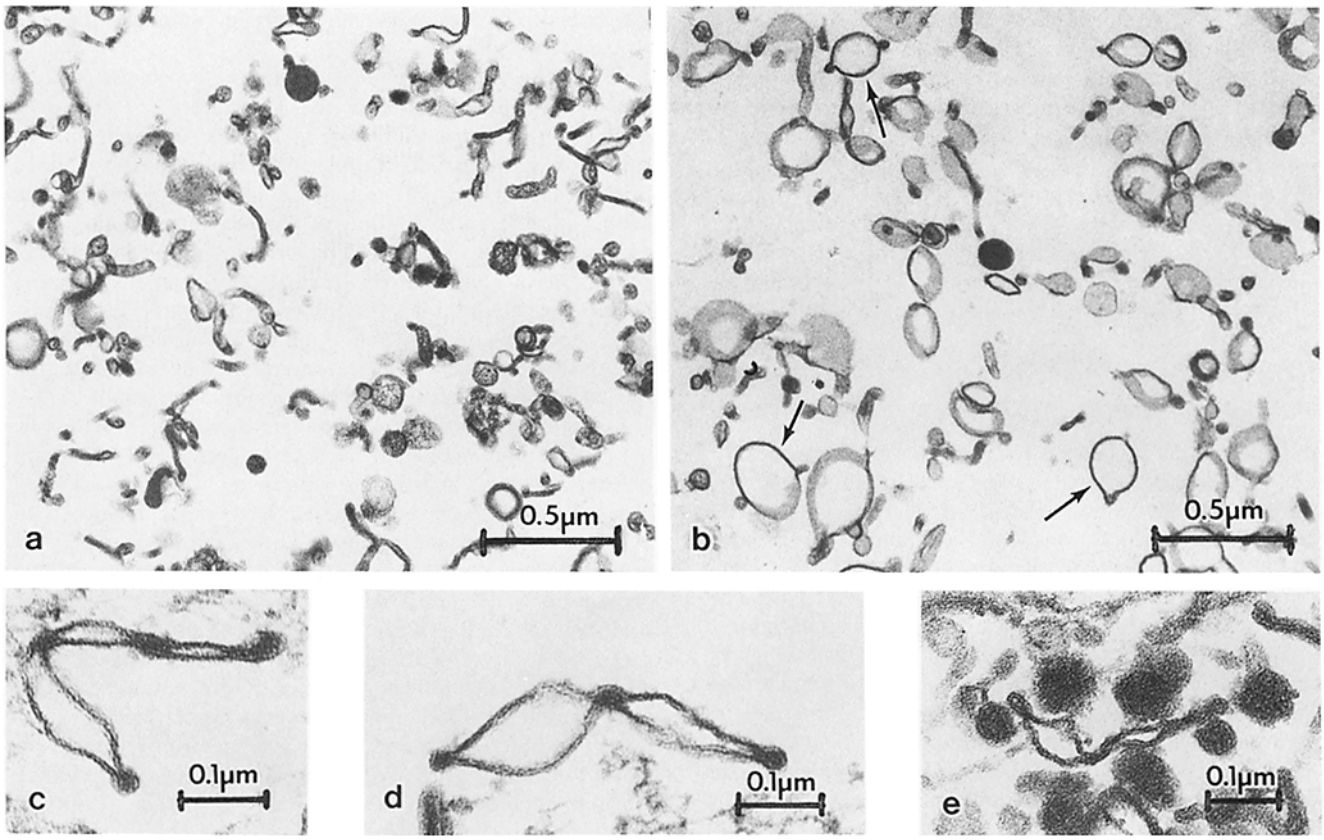

FIGURE 8 Swelling of the transverse tubule due to KCl osmotic imbalance. Stage 1 triad material (prepared by isopycnic centrifugation (21) with no salt treatment) was preincubated in 50% sucrose (wt/wt) containing 0.7 M KCl for 1 h and then underlayed in a step sucrose gradient (10%, 25%, 35%) in an SW 27 tube containing 0.7 M KCl (*a*) or lacking it (*b*). Samples were centrifuged for 1.5 h at 27,000 rpm. Free t-tubule, enriched at the 25/35% sucrose interface, was collected and directly *prefixed* for electron microscopy as described in Materials and Methods. (*a*) Fraction obtained from sucrose gradient containing 0.7 M KCl (i.e. only sucrose osmotic imbalance). × 35,000. (*b*) Fraction obtained from gradient devoid of KCl (KCl and sucrose osmotic imbalance). × 35,000. Note the swollen appearance of the t-tubule in *b* vs *a*. (*c* and *d*) Electron-dense material at intervals of ~0.15 μm within isolated transverse tubule. The latter were prepared from triads. × 120,000. (*e*) Electron-dense matter can also be observed in the transverse tubule of isolated triads. Triad consisting of an extended transverse tubule with multiple associated terminal cisternae (Stage I, *standard* variant). × 100,000.

both by thin section and negative staining that the junctional feet are more tightly associated with the terminal cisternae than the transverse tubule, in keeping with previous observations by Franzini-Armstrong (4) and Campbell et al. (31) by thin-section electron microscopy.

Negative staining clearly shows that the junctional surface of the terminal cisternae is distinct from the remainder of the sarcoplasmic reticulum membrane since the surface appears to be devoid of the characteristic 30–40-Å surface particles referable to calcium pump protein, the major component of the sarcoplasmic reticulum membrane (27). These conclusions are in keeping with the recent histochemical studies of Jorgensen et al. (32).

The difference is further supported by freeze-fracture, which shows a predominant blocklike appearance of the membrane of the junctional face of the terminal cisternae (Fig. 3*a*). The blocks have a periodicity of 250–300Å and may be an integral part of the membrane. Kelly and Kuda (33) have reported the presence of cubelike structures observed in situ by freeze-fracture mainly on the e face. The rectangular blocklike structures described here are more clearly associated with the p face. There is the further suggestion from freeze-fracture that they may consist of subunits (Figs. 3*a* and 4*e*). The width of the structure normal to the plane of the membrane is ~140 Å, or more than two times the width of a phospholipid bilayer. Even if this structure were transmembrane, a major portion would extend out into the gap from the junctional face. The similar periodicity and extension from the surface might be suggestive that these structures, observed by freeze-fracture (Fig. 4), are in part, related to the feet observed by thin section and negative staining.

Freeze-fracture reveals two other types of junctional material: t-tubule associated intragap structures, and interjunctional structures (34) that appear to directly connect the terminal cisternae with transverse tubules (see especially Fig. 4*a*) and might be related to structures reported in situ in thin sectioned material (13, 35, 36). The intragap particles appear preferentially associated with the transverse tubule (Fig. 4*b* and *c*). Thus far, freeze-fracture is the only method of sample preparation that unambiguously reveals particles preferentially associated with the transverse tubule (see also references 8, 37). The association of particles with t-tubules is most likely a reflection of the method of sample preparation. The relationship of such intragap structures to the blocklike structures is uncertain, although there is the suggestion from freeze-fracture of the tissue (Fig. 4*e*) that there is a pairing of the two types of structures (see also reference 8).

The negative staining and freeze-fracture views of isolated

triads presented here are the first of their type and provide new insights and approaches to the study of the triad junction. Both methods display new suggestions of subunit composition of the junctional structures. The availability of isolated triads decreased complications due to the presence of the rest of the myoplasm.

In general, the major features observed in isolated triads can be identified in situ and vice versa. Such similarity in appearance provides some encouragement that the isolated triads, or some variant thereof, may prove useful in the study of the Ca^{++}-release process related to excitation-contraction coupling.

Susceptibility of Triad Morphology to Salt Treatment or Osmotic Influence

Skeletal muscle subcellular fractionation of membranes frequently employs KCl or chaotropic agents such as LiBr (38–40) to disaggregate contractile elements. The use of 0.7 M KCl in our early attempts (21) was found to disrupt triad morphology (Fig. 7), despite apparent purification based on enzymic criteria (1). The studies described here suggest that KCl at least in part extracts the junctional feet. Evidence for salt-induced disruption of feet attached to heavy SR has previously been reported (31). A recent study (26) has questioned whether KCl extracts feet material. Our studies show that the length of exposure to KCl is an important variable.

High salt also induces a second type of alteration of the triads. It causes swelling and loss of osmiophilic contents from the terminal cisternae. Our use of relatively low levels of pyrophosphate (20 mM) to extract contractile material during isolation (1) is less damaging to triad structure than are high KCl concentrations, particularly at the junction.

As a consequence of the pyrophosphate treatment, the terminal cisternae become somewhat swollen and their contents appear less densely packed than in situ. In comparable fractions that have not been exposed to pyrophosphate (Stage I, *standard* preparation) (Figs. 1 *b* and *c* and 6), the terminal cisternae have a somewhat shrunken and condensed appearance. The contents of the terminal cisternae of pyrophosphate-treated triads also become preferentially segregated in regions that appose t-tubule. These patches are also seen on terminal cisternae that are no longer junctionally associated, but that still retain feet. While some of this difference might reflect the influence of the pyrophosphate mixture on osmium staining, it would seem that some partial loss and/or rearrangement of the contents of the terminal cisternae has occurred. Segregation of the contents of the terminal cisternae has also been reported by Caswell et al. (25) with less purified fractions. Purified sarcoplasmic reticulum has been fractionated into heavy and light fractions which are referable to terminal cisternae and lateral cisternae, respectively (41). The luminal contents have been shown to consist mainly of calcium binding protein (41, 42), also termed calsequestrin (43).

Preferential swelling of transverse tubule of striated muscle has been studied extensively (44–47) and forms the basis for a method (glycerol treatment) to detach transverse tubule from surface sarcolemma in situ (48–50). In intact muscle fibers, the transverse tubule component of the triad selectively swells by simple replacement of the external medium with hypertonic solutions of either sucrose or salt (47). The added solutes enter the t-system via the transverse tubule "mouth" or caveolae, causing an osmotic imbalance between the cytoplasmic compartment and lumen of the tubule. This imbalance leads to an osmotic flow of water from the cytoplasm into the tubule, which proceeds faster than the re-exit of water via the constricted tubule mouth.

Transverse tubule swelling in response to osmotic changes can also be demonstrated in the isolated triad structure by electron microscopy. A period of time is necessary for the sucrose or salt to permeate across the tubule membrane. Such long-term preincubation of triads followed by rapid dilution results in preferential swelling of the transverse tubule due to an osmotic inrush of water. The same effect is seen with sucrose or KCl as a solute, except that KCl appears to be more permeable, requiring less time to equilibrate across the transverse tubule membrane. The terminal cisternae are much less sensitive to such osmotic perturbation, undoubtedly reflecting the higher permeability of the SR membrane to solutes (51).

Isolated transverse tubule appears to contain osmiophilic material within the compartment, most prominently at its tips (references 22, 52, and the present report), which do not swell in response to osmotic perturbation. Early morphological data of insect or spider skeletal muscle, either freeze-etched (7, 53) or in thin section (53), indicated that the transverse tubule contains periodic (~0.3 μm) constrictions and dilations. A similar outpocketing of junctional t-tubule has also been proposed by Kelly (54) for immature amphibian muscle. Such dilations have not been reported in situ for adult vertebrate muscle although intraluminal contents with periodicities similar to that observed for feet have been detected (references 26, 55, and this report, Fig. 1 *a*). The isolation procedure results in apparent aggregation of this material (Fig. 8). The identity of such contents remains unexplored.

The ultimate purpose for the isolation of triads was to simplify and make possible the study of excitation-contraction coupling related phenomena in the test tube. Accordingly, it is essential that conditions for isolation be optimized to provide maximal retention of structural and functional characteristics. The susceptibility of triads to a variety of conditions to which they are fragile must be considered in the further refinement of procedures to optimize their isolation or to establish assays to study the Ca^{++}-release process. The studies presented here provide morphological characterization of the triad junction by three different methods of sample preparation and provide new insight into triad ultrastructure. The studies indicate that much of the detail has been preserved, including the junctional structures or feet through which the signal for Ca^{++} release may be transmitted.

The authors wish to acknowledge the technical assistance of Reiko Saito in electron microscopy preparation and the secretarial help of Macie Schreiber.

This work was supported by National Institutes of Health grant AM 14632 and a Muscular Dystrophy Association grant to S. Fleischer and an American Heart Association, Tennessee Affiliate Grant-in-Aid award to P. Palade and R. D. Mitchell. Postdoctoral Fellowship to R. D. Mitchell was provided by the Muscular Dystrophy Association and to P. Palade by U. S. Public Health Service SF32 AM 06386-02.

Received for publication 14 June 1982, and in revised form 7 January 1983.

REFERENCES

1. Mitchell, R. D., P. Palade, and S. Fleischer. 1983. Purification of morphologically intact triad structures from skeletal muscle. *J. Cell Biol.* 96:1008–1016.
2. Porter, K. R., and G. E. Palade. 1957. Studies on the endoplasmic reticulum. III. Its form and distribution in striated muscle cells. *J. Biophys. Biochem. Cytol.* 3:269–300.
3. Peachey, L. D. 1965. The sarcoplasmic reticulum and transverse tubules of the frog's sartorius. *J. Cell. Biol.* 25:209–231.
4. Franzini-Armstrong, C., 1970. Studies of the triad. I. Structure of the junction in frog twitch fibers. *J. Cell Biol.* 47:488–499.

5. Endo, M. 1977. Calcium release from the sarcoplasmic reticulum. *Physiol. Rev.* 57:71–108.
6. Revel, J. P. 1962. The sarcoplasmic reticulum of the bat cricothyroid muscle. *J. Cell Biol.* 12:571–588.
7. Franzini-Armstrong, C. 1974. Freeze fracture of skeletal muscle from the tarantula spider. *J. Cell. Biol.* 61:501–513
8. Franzini-Armstrong, C. 1975. Membrane particles and transmission at the triad. *Fed. Proc.* 34:1382–1389.
9. Bianchi, C. P., and T. C. Bolton. 1967. Action of local anesthetics on coupling systems in muscle. *J. Pharmacol. Exp. Ther.* 157:388–405.
10. Ebashi, S., and M. Endo. 1968. Calcium ion and muscle contraction. *Prog. Biophys. Mol. Biol.* 18:123–183.
11. Franzini-Armstrong, C. 1971. Studies of the triad. II. Penetration of tracers into the junctional gap. *J. Cell Biol.* 49:196–203.
12. Mathias, R., R. A. Levis, and R. S. Eisenberg. 1980. Electrical models of excitation-contraction coupling and charge movement in skeletal muscle. *J. Gen. Physiol.* 76:1–31.
13. Somlyo, A. V. 1979. Bridging structures spanning the junctional gap at the triad of skeletal muscle. *J. Cell. Biol.* 80:743–750.
14. Schneider, M. F., and W. K. Chandler. 1973. Voltage dependent charge movement in skeletal muscle: a possible step in excitation-contraction coupling. *Nature (Lond.).* 242:244–246.
15. Fleischer, S., B. Fleischer, and W. Stoeckenius. 1967. Fine structure in lipid-depleted mitochondria. *J. Cell Biol.* 32:193–208.
16. Sato, T. 1968. A modified method for lead staining of thin sections. *J. Electron Microsc.* 17:158–159.
17. Deamer, D. W., and R. J. Baskin. 1969. Ultrastructure of sarcoplasmic reticulum preparations. *J. Cell Biol.* 42:296–307.
18. Peachey, L. D., and B. R. Eisenberg. 1978. Helicoids in the T system and striations of frog skeletal muscle fibers seen by high voltage electron microscopy. *Biophys. J.* 22:145–154.
19. Luff, A. R., and H. L. Atwood. 1971. Changes in the sarcoplasmic reticulum and transverse tubular system of fast and slow skeletal muscle of the mouse during postnatal development. *J. Cell Biol.* 51:369–383.
20. Packer, L., C. W. Mehard, G. Meissner, W. L. Zahler, and S. Fleischer. 1974. The structural role of lipids in mitochondrial and sarcoplasmic reticulum membranes. Freeze-fracture electron microscopy studies. *Biochim. Biophys. Acta.* 363:159–181.
21. Mitchell, R. D. 1981. Initial studies in excitation-contraction coupling: isolation and characterization of the triad structure from skeletal muscle. Nashville, TN: Vanderbilt University. Dissertation 1–274.
22. Lau, Y. H., A. H. Caswell, and J.-P. Brunschwig. 1977. Isolation of transverse tubule by fractionation of triad junctions of skeletal muscle. *J. Biol. Chem.* 252:5565–5574.
23. Schiaffino, S., V. Hanzlikova, and S. Pierobon. 1970. Relations between structure and function in rat skeletal muscle fibers. *J. Cell Biol.* 47:107–119.
24. Caswell, A. H., Y. H. Lau, M. Garcia, and J.-P. Brunschwig. 1979. Recognition and junction formation by isolated transverse tubules and terminal cisternae of skeletal muscle. *J. Biol. Chem.* 254:202–208.
25. Caswell, A. H., Y. H. Lau, and J.-P. Brunschwig. 1976. Ouabain binding vesicles from skeletal muscle. *Arch. Biochem. Biophys.* 176:417–430.
26. Brunschwig, J. P., N. Brandt, A. H. Caswell, and D. S. Lukeman. 1982. Ultrastructural observations of isolated and fragmented junctions of skeletal muscle by use of tannic acid mordanting. *J. Cell Biol.* 93:533–542.
27. Saito, A., C.-T. Wang, and S. Fleischer. 1978. Membrane asymmetry and fast enhanced ultrastructural detail of sarcoplasmic reticulum revealed with use of tannic acid. *J. Cell Biol.* 79:601–616.
28. Franzini-Armstrong, C. 1973. Studies of the triad. IV. Structure of the junction in frog slow fibers. *J. Cell Biol.* 56:120–128.
29. Walker, S. M., G. R. Schrodt, G. J. Currier, and E. V. Turner. 1975. Relationship of sarcoplasmic reticulum to fibril and triadic junction development in skeletal muscle fibers of fetal monkeys and humans. *J. Morphol.* 146:97–128.
30. Walker, S. M., G. R. Schrodt, G. J. Currier, and J. W. Yuen. 1975. Development of the triadic junction in skeletal muscle fibers of fetal and postnatal rats. *Am. J. Phys. Med.* 54:61–79.
31. Campbell, K. P., C. Franzini-Armstrong, and A. Shamoo. 1980. Further characterization of light and heavy sarcoplasmic reticulum vesicles. Identification of the 'sarcoplasmic feet' associated with heavy sarcoplasmic reticulum vesicles. *Biochim. Biophys. Acta.* 602:97–116.
32. Jorgensen, A. O., A. C. Y. Shen, D. H. MacLennan, and K. T. Tokuyasu. 1982. Ultrastructural localization of the Ca^{2+} + Mg^{2+}-dependent ATPase of sarcoplasmic reticulum in rat skeletal muscle by immunoferritin labeling of ultrathin frozen sections. *J. Cell Biol.* 92:409–416.
33. Kelly, D. E., and A. E. Kuda. 1979. Subunits of the triadic junction in fast skeletal muscle as revealed by freeze-fracture. *J. Ultrastruct. Res.* 68:220–233.
34. Rayns, D. G., C. E. Devine, and C. L. Sutherland. 1975. Freeze fracture studies of membrane systems in vertebrate muscle. I. Striated muscle. *J. Ultrastruct. Res.* 50:306–321.
35. Eisenberg, B. R., and A. Gilai. 1979. Structural changes in single muscle fibers after stimulation at a low frequency. *J. Gen. Physiol.* 74:1–16.
36. Eisenberg, B. R., and R. S. Eisenberg. 1982. The T-SR junction in contracting single skeletal muscle fibers. *J. Gen. Physiol.* 79:1–19.
37. Franzini-Armstrong, C. 1980. Structure of sarcoplasmic reticulum. *Fed. Proc.* 39:2403–2409.
38. Kono, T., and S. P. Colowick. 1961. Isolation of skeletal muscle cell membrane and some of its properties. *Arch. Biochem. Biophys.* 93:520–533.
39. Martonosi, A. 1968. Sarcoplasmic reticulum. IV. Solubilization of microsomal adenosine triphosphatase. *J. Biol. Chem.* 243:71–81.
40. Barchi, R. L., J. B. Weigele, D. M. Chalikian, and L. E. Murphy. 1979. Muscle surface membranes: preparative methods affect apparent chemical properties and neurotoxin binding. *Biochim. Biophys. Acta.* 550:59–76.
41. Meissner, G. 1975. Isolation and characterization of two types of sarcoplasmic reticulum vesicles. *Biochim. Biophys. Acta.* 389:51–68.
42. Fleischer, S., C.-T. Wang, A. Saito, M. Pilarska, and J. O. McIntyre. 1979. Structural Studies of Sarcoplasmic Reticulum *in vitro* and *in situ*. *In Cation Flux Across Biomembranes*. Y. Mukohata and L. Packer, editors. Academic Press, New York. 193–205.
43. MacLennan, D. H., and P. T. S. Wong. 1971. Isolation of a calcium-sequestering protein from sarcoplasmic reticulum. *Proc. Natl. Acad. Sci. U. S. A.* 68:1231–1235.
44. Foulks, J. G., J. A. Pacey, and F. A. Perry. 1965. Contractures and swelling of the transverse tubules during chloride withdrawal in frog skeletal muscle. *J. Physiol. (Lond.).* 180:96–115.
45. Rapoport, S. I., L. D. Peachey, and D. A. Goldstein. 1969. Swelling of the transverse tubular system in frog sartorius. *J. Gen. Physiol.* 54:166–177.
46. Birks, R., and D. F. Davey. 1972. An analysis of volume changes in the T-tubes of frog skeletal muscle exposed to sucrose. *J. Physiol. (Lond.).* 222:95–111.
47. Franzini-Armstrong, C., J. E. Heuser, T. S. Reese, A. P. Somlyo, and A. V. Somlyo. 1978. T-tubule swelling in hypertonic solutions: a freeze substitution study. *J. Physiol. (Lond.).* 283:133–140.
48. Howell, J. N., and D. J. Jenden. 1967. T-tubules of skeletal muscle: morphological alterations which interupt excitation-contraction coupling. *Fed. Proc.* 26:553.
49. Eisenberg, R. S., and P. W. Gage. 1967. Changes in the electrical properties of frog skeletal muscle fibers after disruptions of the transverse tubular system. *Science (Wash. D.C.).* 158:1700.
50. Davey, D. F., A. F. Dulhunty, and D. Fatkin. 1980. Glycerol treatment in mammalian skeletal muscle. *J. Membr. Biol.* 53:223–234.
51. Kometani, T., and M. Kasai. 1978. Ionic permeability of sarcoplasmic reticulum vesicles measured by light scattering method. *J. Membr. Biol.* 41:295–308.
52. Lau, Y. H., A. H. Caswell, J.-P. Brunschwig, R. J. Baerwald, and M. Garcia. 1979. Lipid analysis and freeze-fracture studies on isolated transverse tubules and sarcoplasmic reticulum subfractions of skeletal muscle. *J. Biol. Chem.* 254:540–546.
53. Smith, D. S., and H. C. Aldrich. 1971. Membrane systems of freeze-etched striated muscle. *Tissue & Cell.* 3:261–281.
54. Kelly, D. E. 1969. The fine structure of skeletal muscle triad junctions. *J. Ultrastruct. Res.* 29:37–49.
55. Bonilla, E. 1977. Staining of transverse tubular system of skeletal muscle by tannic acid-glutaraldehyde fixation. *J. Ultrastruct. Res.* 58:162–165.